explaining and predicting
the ocean conveyor

D1.1 Paleo Proxy Records

Details of new and existing paleo proxy records collated for feeding into other tasks

Date: 2023/12/19

Authors: Jack Wharton & David Thornalley

Funded by
the European Union

EPOC – Explaining and Predicting the Ocean Conveyor – is funded by the European Union.
Views and opinions expressed are however those of the author(s) only and do not necessarily reflect those of the European Union.
Neither the European Union nor the granting authority can be held responsible for them.

Document information sheet

EU Project No.	101059547	**Acronym:**	EPOC
Project title:	Explaining and Predicting the Ocean Conveyor		
Project website:	www.epoc-eu.org		
Title:	D1.1 (D14) Paleo Proxy Records		
Work Package:	WP1: Quantifying Past AMOC changes		
Responsible partner:	UCL		
Date of delivery:	Contractual: 31 Dec 2023	Actual: 21 Dec 2023	
Dissemination level:	PU – Public, fully open		

Author(s) ***Contact:*** *epoc-admin@uni-hamburg.de*	**Institution**
Jack Wharton	UCL
David Thornalley	UCL

Document version log *Draft: 0.X; First submission 1.X; Second submission 2.X*			
Version #	Date	Comment	Authors
0.5	21.11.2023	Drafts	Jack Wharton, David Thornalley
0.6	29.11.2023	Internal review	Jon Robson
0.7	09.12.2023	Revised version after internal review	Jack Wharton, David Thornalley
1.0	18.12.2023	Final version	Jack Wharton, David Thornalley
1.0	19.12.2023	D1.1 version submitted to EC Portal	Kaja Scheliga

Paleo Proxy Records

1 Introduction

The Atlantic Meridional Overturning Circulation (AMOC) is a key component of the Earth's climate system, which involves the transport of warm and saline surface waters northward into the high latitude North Atlantic, where they cool, sink and flow back southwards at depth (Buckley & Marshall, 2016). Northward surface transport is primarily by the Gulf Stream and its more northerly extension, the North Atlantic Current, which flows northeast across the Atlantic after the Gulf Stream separates from the North American coast east of Cape Hatteras. Much of the southward return flow at depth occurs via the Deep Western Boundary Current (DWBC), which carries so-called North Atlantic Deep Waters (NADW) formed in the subpolar North Atlantic along the western continental margin of the North Atlantic into the South Atlantic. Monitoring of the AMOC over the past two decades suggests the AMOC has weakened at a rate of ~0.1 Sv/yr (Srokosz & Bryden, 2015; Moat et al., 2023), however, since these observations are limited to the last ~20 years, proxy based reconstructions are necessary to place these observations into a longer-term context, i.e., is this weakening part of a long-term trend or are these changes representative of natural variability?

While numerous previous independent AMOC reconstructions using different proxies suggest that the observed current weakening is part of a longer-term trend starting approximately 150 years ago (Caesar *et al.,* 2021), there are inconsistencies between various paleo and modern proxies (Thornalley *et al.,* 2018; Moffa-Sanchez *et al.,* 2019), as well as paleo proxies and coupled models (Menary *et al.,* 2020). To address these issues, EPOC will perform a systematic re-evaluation of different proxies used to reconstruct AMOC variability by compiling new and published paleoceanographic proxy records that are either directly and/or indirectly related to AMOC and comparing them to a suite of different AMOC transport simulations. Quantitative methods such as correlation and regression will then be used to evaluate each AMOC proxies' utility and robustness. EPOC is also focused on quantifying and explaining past AMOC changes, including an assessment of the meridional and vertical coherence of the DWBC over the last ~10,000 years (a period of time known as the Holocene), with a particular focus on the last 1000 years (henceforth, last ~1 ka).

Previous work by Moffa-Sanchez *et al.,* (2019) and Caesar *et al.,* (2021) have already compiled numerous paleoceanographic proxy data, however, many new records have been published since then and there is also a distinct lack of deep ocean records within these existing syntheses, especially those corresponding to the DWBC. Therefore, to address this issue, as part of EPOC, we have generated new records from the deep ocean at a range of latitudes and ocean depths, all of which correspond to the DWBC and its constituent currents. This includes flow speed records derived from the sortable silt mean grain size proxy (SS), as well as other proxies such as benthic foraminiferal $\delta^{18}O_c$, the latter of which is primarily controlled by temperature in the North Atlantic over the last millennium. While these new records feed directly into our new and updated compilation of AMOC proxy records, we also present and provide an examination of these new proxy records, which also allows us to assess the DWBC's meridional and vertical coherence.

The structure of this report is as follows: Section 2 presents a combination of newly generated and published grain size records from several locations along the path of the southward flowing DWBC. We divide these records into three sections based on which of the DWBC's constituent water masses they most likely reflect, i.e., Labrador Sea Water (LSW), Iceland-Scotland Overflow Water (ISOW), and Denmark Strait Overflow Water (DSOW), although as we note throughout, (1) the average depth of

these water masses may have varied throughout the Holocene, and (2) other water masses, e.g., Antarctic Bottom Water (AABW) may also partly influence some sites. In Section 3 we present new benthic foraminiferal $\delta^{18}O_c$ records from some of the same sites spanning the last 1ka, and in Section 4 we summarise the main findings of this report, as well as the main findings from previous syntheses. Finally, an accompanying excel file "AMOC proxy records", contains the raw data corresponding to the records presented in this document, collated alongside other proxy records from the North Atlantic, for delivery to WP3 in fulfilment of Milestone 2.

2 Sortable silt mean grain size records

2.1 Labrador Sea Water (LSW)

LSW is an intermediate depth water mass and the shallowest component of the DWBC (~1-2.5 km). It is formed via cooling, densification, and sinking of subpolar mode waters in the Iceland and Irminger Seas during winter, with additional dense water production and modification occurring downstream in the Labrador Sea (Petit *et al.,* 2020). While sediment cores from these depths in the Northwest Atlantic are bathed by LSW, they may also be influenced by shallower near-surface currents, which can penetrate down to ~1 km water depth. This includes: (1) the warm and saline northward flowing Gulf Stream and its associated jets and meanders, and (2) the more inshore and southward flowing shelfbreak jet system, which is typically much colder and fresher due to its subpolar origin.

Previous proxy and modelling work suggests LSW has undergone a long-term increase over the last ~8 ka, likely in response to surface cooling in the Labrador Sea and/or a reduction of Nordic Seas overflow waters at LSW depths (Renssen *et al.,* 2005; Hoffmann *et al.,* 2019). Super imposed on this long-term trend, hydrographic proxy reconstructions also suggest that LSW has undergone millennial scale variability, which coincide with periods of increased drift ice and regional glacier advances (Marchitto & deMenocal, 2003). And on more recent timescales, flow speed reconstructions suggest a reversal of the long-term increase, with slower inferred flow speeds during the 20th Century (Thornalley *et al.,* 2018). Here, we present and examine a selection of new and published flow speed records from multiple locations along the path of the DWBC that are predominantly bathed by LSW (Table 1; Figure 1). We further divide the records presented in this section between those spanning the last 1 ka and last 8 ka, with 8 ka marking the approximate time when LSW was first established after the final melting of the Laurentide Ice Sheet (Hoogakker *et al.,* 2011).

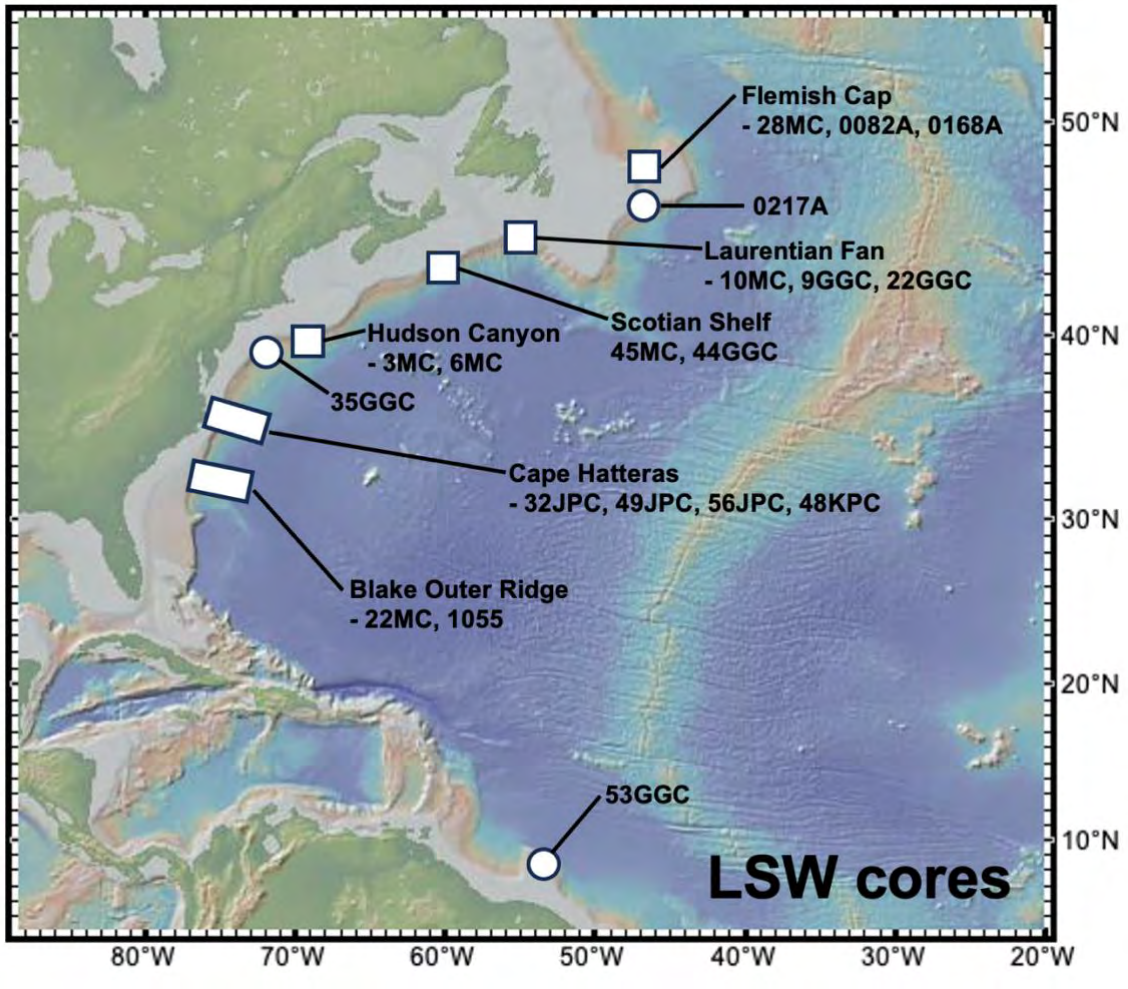

Figure 1. Site map showing location of cores detailed in Table 1. Circles denote single cores, squares denote multiple cores, and rectangles denote paleoenvironmental depth transects.

Table 1. Details of cores corresponding to typical LSW depths.

Core and (abbreviation)	Region	Lat. (N)	Long. (W)	Depth (m)	Duration	Reference
KNR-158-28MC-X (28MC)		49.24	48.99	1828	8 ka	Hoffmann *et al.*, 2019
MO-2009061-0082A (82A)	Flemish Pass	48.22	47.03	1450	1 ka	This report
MO-2009061-0168A (168A)	Flemish Pass	47.99	46.66	960	1 ka	Piper *et al.*, 2021
MO-2009061-0217A (217A)	Flemish Pass	46.39	46.74	1195	1 ka	Rashid *et al.*, 2023
OCE-326-22GGC (22GGC)	Laurentian Fan	44.68	55.25	1357	8 ka	This report
KNR-158-10MC-Y (10MC)	Laurentian Fan	44.82	54.90	1854	1 ka	This report

KNR-158-9GGC (9GGC)	Laurentian Fan	44.83	54.90	1854	8 ka	This report
KNR-197-45MC-C (45MC)	Scotian Shelf	43.35	60.21	966	1 ka	O'Brien *et al.*, 2021
KNR-197-44GGC (44GGC)	Scotian Shelf	43.35	60.21	966	8 ka	This report
AR36-3MC-C (3MC)	Hudson Canyon	39.28	72.17	665	8 ka	This report
AR36-MC6-C (6MC)	Hudson Canyon	39.24	72.12	957	8 ka	This report
KNR-198-35GGC (35GGC)	Line W	39.87	68.98	1824	8 ka	This report
KNR-178-32JPC (32JPC)	Cape Hatteras	35.98	74.71	1006	8 ka	This report
KNR-178-49JPC (49JPC)	Cape Hatteras	35.76	74.44	1515	1 ka/8 ka	This report
KNR-178-56JPC (56JPC)	Cape Hatteras	35.46	74.71	1731	1 ka	Thornalley *et al.*, 2018
KNR-178-48JPC (48JPC)	Cape Hatteras	35.76	74.44	2009	1 ka/8 ka	Thornalley *et al.*, 2018
CH07-98-22MC-B (22MC)	Carolina Slope	32.78	76.27	1895	1 ka	This report
ODP-172-1055 (1055)	Caroline Slope	32.78	76.28	1798	8 ka	This report
KNR-197-53GGC (53GGC)	Dem. Rise	8.23	53.23	1272	8 ka	This report

2.1.1 Last 1 ka

This compilation of cores examining LSW variability over the last 1 ka show a range of different behaviour between ~1000 and ~1800 CE. In particular, many cores show notable Industrial-Era changes, which are broadly consistent with suggested regime shifts in surface and deep ocean circulation in the North Atlantic starting at ~1850 CE (Keigwin et al., 2003; Moore et al., 2017; Lower-Spies et al., 2020; Spooner et al., 2020). The grain size data for cores spanning the last 1 ka are shown in Figure 2 and the key results are as follows:

- All three Flemish Pass records exhibit similar behaviour over the last ~1 ka (Figure 2a; Piper et al., 2021; Rashid et al., 2023). They remain relatively constant until 1500 CE, followed by a trend towards faster flow and greater variability over the last ~500 years, with fastest inferred flow speeds during the 20th Century.
- Further downstream, 45MC and 10MC are situated at depths currently bathed by the upper and lower layers of LSW respectively, making them ideally situated to evaluate the vertical coherence of LSW (Figure 2b).

- Shallow site 45MC reveals a relatively gradual shift to slower flow between 1000 CE and 1800 CE, followed by an abrupt shift to faster flow speeds post ~1800 CE, whereas deeper site 10MC is characterized by a slight increase in flow speeds over the first ~800 years and a more muted change than 45MC at 1800 CE.
- These seemingly opposing results suggest that either there were vertical migrations in the depth of LSW over the last ~ 1 ka, or the local bathymetry – including the sharp concave corner near the outflow of the Laurentian Channel, may be causing local circulation patterns which mask any coherence in the along-slope flow of the DWBC. Assessing the vertical coherence of LSW is a key target for testing in model simulations as part of WP3.
- Cape Hatteras sites 56JPC and 48JPC show similar behaviour over the last ~1 ka (Thornalley et al., 2018) and good agreement with shallower site 49JPC at 1500-1800 CE (Figure 2c).
- However, between 1200 and 1500 CE, 48JPC and 49JPC show different behaviour, which (based on δ18Oc data [see section 3]) may be related to a shoaling of DWBC and/or weakening (strengthening) of denser (lighter) LSW.
- Since previous work investigated changes in the DWBC using a relatively low resolution model and homogenous DWBC (Thornalley et al., 2018), these inferred differences between cores retrieved from similar depths present a key target for future work, namely exploring how easily different trends at different depths may related to vertical versus latitudinal differences in the DWBC flow speeds.
- Finally, by exhibiting opposite behaviour to 56JPC and 48JPC, Carolina Slope core 22MC also marks a key target for future modelling work (Figure 2d).

In addition to Flemish Pass core 82A (Figure 2a), we have also dated and measured SS in two other cores from the Flemish Pass region (MO-2009061-0210A and MO-2010061-Ph1-0058A). However, there are large differences in the inferred ages from ^{210}Pb and ^{14}C, most likely due to the impact of bioturbation on the ^{210}Pb records (we also note that the SS records in these cores are likely impacted by bioturbation too). To circumvent this issue and retrieve the original ^{210}Pb, we have developed a diffusive-based bioturbation mixing model, which can account for the effects of bioturbation and produce an alternative age model that is consistent with coeval ^{14}C data (Girard-Sequeira, 2023; MSc thesis). This model is also able to deconvolve the effects of bioturbation on SS records, i.e., smoothing and reduction in the amplitude of variability. Application of this model to the two additional Flemish Pass cores helps reconcile ^{210}Pb and ^{14}C dates and produces SS results that are consistent with other nearby cores, e.g., 82A, better resolving recent changes in SS since ~1900 CE. Given the success of this modelling approach, similar work will be undertaken on other cores from the region that may also have been Impact by bioturbation, e.g., 217A (Rashid *et al.,* 2023) and 45MC.

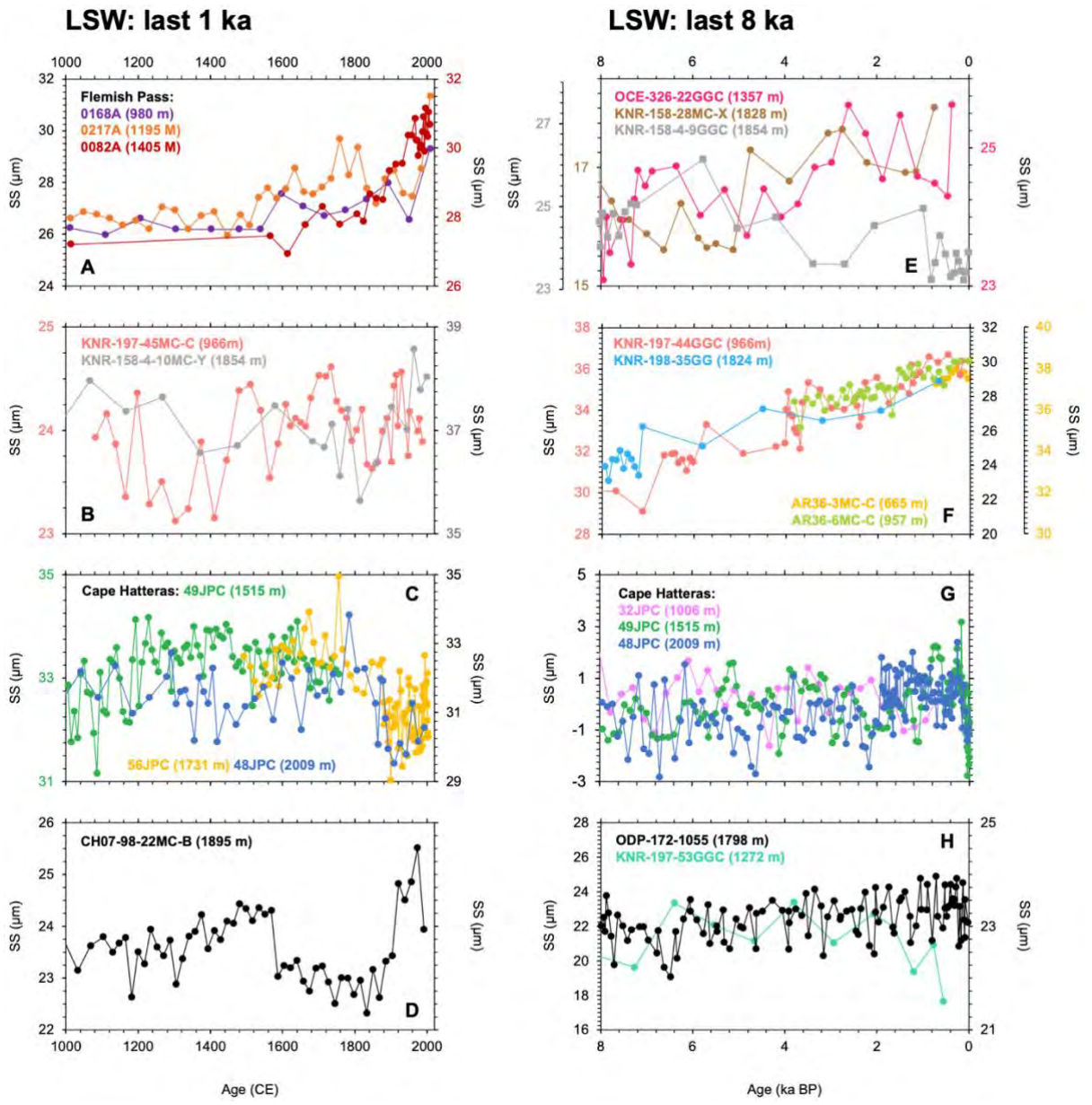

Figure 2. Compilation of grain size records from cores predominantly influenced by LSW for the last ~1 ka (left panels) and last ~8 ka (right panels). (a) Flemish Pass – 0082A (dark red), 0217A (orange; Rashid et al., 2023), & 0168A (purple; Piper et al., 2021); (b) Scotian Shelf – 45MC-C (light red) & Laurentian Fan -10MC-Y (grey); (c) Cape Hatteras – 49JPC (green), 56JPC (yellow), & 48JPC (blue); (d) Caroline Slope – CH07-98-22MC-B (black); (e) Orphan Basin Slope – 28MC-X (brown; Hoffmann et al., 2019) & Laurentian Fan cores 22GGC (pink)/9GGC (grey); (f) Scotian Shelf – 44GGC (light blue), Line W – 35GGC (light red), Hudson Canyon cores 3MC (tangerine)/6MC (lime); (g) Cape Hatteras – 32JPC (bright pink), 49JPC (green), & 48JPC (blue); (h) Caroline Slope – 1055 (black) & Demerara Rise (turquoise).

Building on the success of this modelling approach, additional work is being undertaken to develop a detailed understanding of the subsurface flow around the Flemish Cap over the last ~1 ka, work which will act as a target for modelling work as part of other EPOC work packages. To do this, we have sampled and resampled a further 10 cores from around Flemish Cap, with some combination of ^{210}Pb, ^{14}C, SS, and planktic and benthic foraminiferal assemblage and geochemical analyses ($\delta^{18}O_c$ and Mg/Ca) planned for each core, dependant on existing work. Core sampling was carried out in person by

UCL PDRA (Jack Wharton) at Bedford Institute of Oceanography, Nova Scotia, Canada in October 2023 and is detailed with sampling notes in in Figure 3.

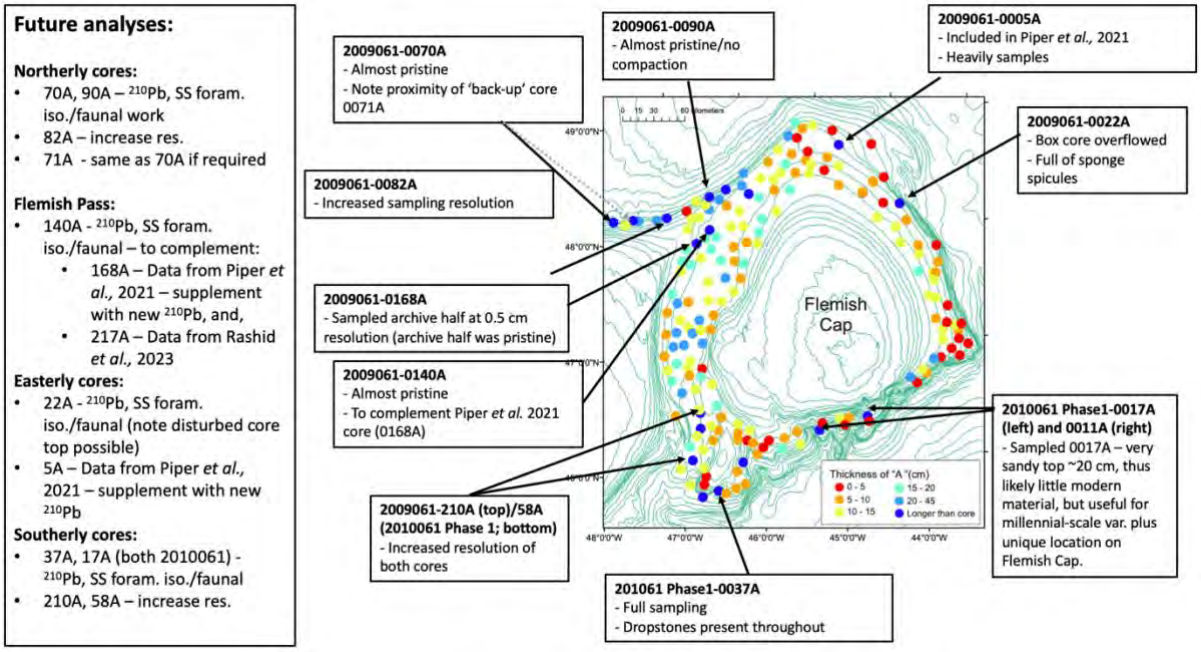

Figure 3. Flemish Cap sampling notes and planned future analyses. Map from Weitzman et al., (2014). Coloured dots denote the thickness of Holocene age sediments. In order to generate the highest resolution records possible we focused our sampling efforts on cores with the thickest Holocene sections (A – blue dots).

2.1.2 Holocene (last ~8 ka)

On millennial timescales, flow speed records corresponding to LSW generally show a long-term increase over the last ~8 ka, behaviour that is consistent with previous modelling work (Renssen *et al.,* 2005) and published Holocene flow speed reconstructions (Hoffmann *et al.,* 2019). While this might suggest that on longer timescales LSW flow speeds are relatively coherent both latitudinally and vertically, this trend is not seen at all core locations, thus it presents a clear target for future modelling work. These data are presented in Figure 2, with a summary of the key results below:

- Laurentian Fan core 22GGC shows good agreement with Orphan Basin Slope core 28MC (Hoffmann *et al.,* 2019), with both records exhibiting a gradual increase over the last ~8 ka (Figure 2e).
- However, 9GGC (from the same site as 10MC [see section 2.1.1]) hints at a long-term decrease over the same time period (Figure 2e), which suggests that either:
    1. At Laurentian Fan, flow speeds are vertically incoherent during the Holocene, or;
    2. 9GGC (and companion core 10MC) is not recording the main axis of LSW flow.
- Scotian Shelf, Hudson Canyon, and 'Line W' cores spanning between 665 m and 1824 m water depth all show a gradual increase over the last ~8 ka (Figure 2f), consistent with upstream sites 28MC and 22GGC, and further highlighting the potentially anomalous nature of 9GGC.
- Cape Hatteras and Blake Outer Ridge cores 48JPC, 49JPC, and 1055 also resolve an increasing trend over the last ~8 ka (Figure 2g and 2h).

- In comparison, KNR-178-32JPC, shows no overall trend during the Holocene, which could be due to the influence of the Gulf Stream, which occupies the water column down to ~1 km above the shelf at Cape Hatteras.
- At Demerara Rise, 53GGC also does not reveal a long-term increase during the Holocene (Figure 2h), however, since this core is sparsely dated and relatively low resolution, additional work improving the age model and increasing the number of grain size measurements are required in order assess the presence of LSW as far south as Demerara Rise in more detail.

2.2 Iceland Scotland Overflow Water (ISOW)

ISOW forms via deep convection in the Nordic Seas and enters the North Atlantic by overflowing the Greenland-Scotland Ridge (GSR) between Iceland and Scotland. As it descends into the Iceland Basin it also entrains large volumes of saltier Subpolar Mode Water (SPMW), which differentiates it from other fresher deep water masses in the subpolar North Atlantic. However, despite ISOW's relative salinity, it is warmer and thus less dense than underlying Denmark Strait Overflow Water (DSOW). While the majority of ISOW is advected westwards through the Charlie Gibbs Fracture Zone and exported out of the North Atlantic as part of the DWBC, emerging work has revealed the presence of multiple interior spreading pathways in the Northeast Atlantic (Lozier *et al.,* 2022). Of particular relevance to comparing ISOW proxy records from different locations along its flow path, is that the downstream version of ISOW, known as Northeast Atlantic Deep Water (NEADW; Lazier *et al.,* 2002), typically occupies the water column between depths of ~2.5 and 3.5 km across the North American continental shelf, whereas ISOW is centred at ~2-2.5 km throughout the Iceland Basin .

Despite early work suggesting ISOW strength was relatively invariable throughout the Holocene (Bianchi & McCave, 1999), a more up to date view is that there has been a long-term decline in ISOW strength over the last ~7 ka due to increased freshwater input into the Nordic Seas, which inhibits deep convection and thus ISOW formation (Thornalley *et al.,* 2013; Kissel *et al.,* 2013; Mjell *et al.,* 2015). These records also exhibit persistent millennial to centennial-scale variability, with periods of weaker ISOW coincident with previously recognised cold climate events when sea-ice production and/or drift-ice export out of the Arctic likely increased, further supporting a strong freshwater-convective control on ISOW variability. Here we present a combination of new, updated, and previously published grain size records from depths and locations currently bathed by ISOW (Table 2; Figure 4). And as in the previous section, we also divide these records between those that span the last 1 ka and Holocene.

Table 2. Details of cores corresponding to typical ISOW/NEADW depths (BOR = Blake Outer Ridge).

Core and (abbreviation)	Region	Lat. (N)	Long. (W)	Depth (m)	Duration	Reference
EN539-14MC-A/B/G (14MC)	South of Iceland	61.35	20.35	2274	1 ka	This report
EN539-16MC-A/B/5P(16MC)	South of Iceland	61.48	19.54	2311	1 ka	This report
GS06-144-9MC-D (9MC)	South of Iceland	60.32	23.97	2081	1 ka	Mjell *et al.,* 2016
RAPiD-21-COM (21COM)	S. Gardar Drift	57.45	27.91	2630	1 ka	Moffa-Sanchez & Hall, 2017
KNR-178-8MC-B/VM24-01 (8MC)	Cape Hatteras	35.86	73.87	2997	1 ka	This report

ISOW stack	South of Iceland	-	-	-	Holocene	Thornalley, in prep.
MD99-2251 (MD2251)	S. Gardar Drift	57.45	27.91	2620	Holocene	Hoogakker *et al.*, 2011
KNR-178-15JPC (15JPC)	Cape Hatteras	35.93	74.11	2626	Holocene	This report
KNR-178-7MC-A/6GGC (7MC)	Cape Hatteras	35.82	73.59	3485	Holocene	This report
KNR-140-39GGC (39GGC)	BOR	31.67	75.42	2975	Holocene	Evans & Hall, 2008
ODP-172-1057 (1057)	BOR	32.03	76.05	2584	Holocene	This report

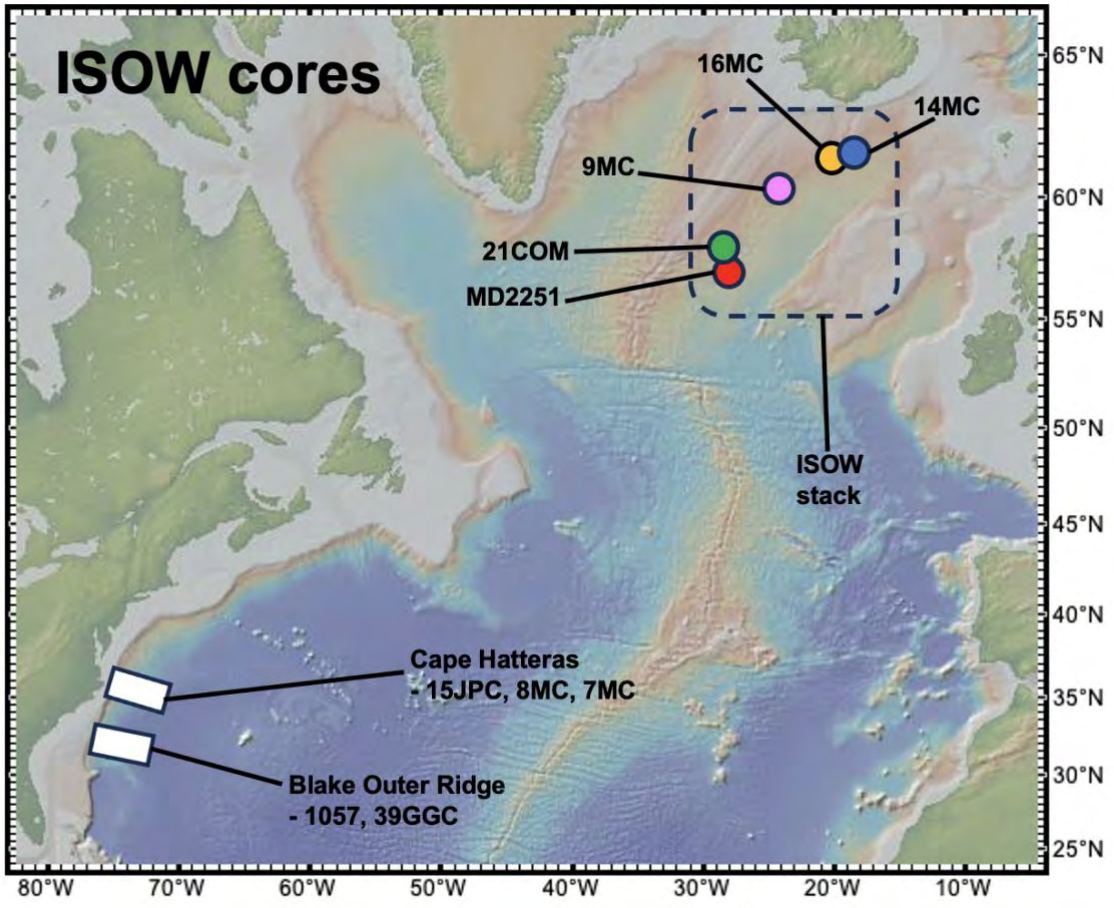

Figure 4. Site map showing location of cores detailed in Table 2. Coloured circles denote single cores, rectangles denote paleoenvironmental depth transects, and dashed box marks the region from which cores in the ISOW stack are located.

2.2.1 Last 1 ka

Multiple grain size records from the Iceland Basin show a major decrease during the Industrial Era, however, the exact timing of the onset of this shift varies between different locations. We also note that grain size records from locations more removed from the main axis of ISOW flow exhibit different behaviour from those located closer, which highlights the importance of site selection in constraining past ISOW variability. In particular, we have multiple grain size records from shallower sites in the Iceland Basin above the main axis of flow, which show little variability and are omitted from this report. These data are presented in Figure 5 and the key results are as follows:

- Iceland Basin core 16MC, located within the main core of ISOW flow (Figure 6), shows a decline beginning at ~1750 CE (Figure 5b; similarly reduced values post ~1750 CE are also seen in a second multicore from the same site, which suggests the signal is robust).
- Nearby Iceland Basin core 14MC, also located within the main core of ISOW (Figure 6), also shows an abrupt shift to smaller values. However, the timing of the onset of this decrease occurs ~100 years later (Figure 5a; like 16MC, the signal is also reproduced in two additional multicores from the same site, which suggests the data is robust).
- Since we see little change in grain size records from shallower depths in the Iceland Basin, we suggest that these grain size changes are caused by a reduction in ISOW strength (although what is causing the difference in timing between 14MC and 16MC is uncertain), rather than a shoaling of ISOW, since the latter would cause variability in grain size records from these shallower cores.
- Further downstream, core site 9MC also exhibits a similarly timed decrease to 16MC (Figure 5c; Mjell *et al.,* 2015), although the magnitude of change is more muted, most likely due to the core's more distal location with respect to the main axis of ISOW flow (Figure 6).
- In comparison, Gardar Drift core 21COM shows no long-term trend over the last ~1 ka (Figure 5d; Moffa-Sanchez & Hall, 2017). This is most likely due to the core's location away from the main flow axis of ISOW, instead influenced by a side-branch of ISOW flow, steered around a local bathymetric feature on Gardar Drift (Figure 6).
- Finally, core 8MC at Cape Hatteras shows similar behaviour to 16MC (Figure 5e), which suggests it is bathed by the downstream product of ISOW and hints at the possibility that ISOW may be coherent latitudinally on centennial timescales.

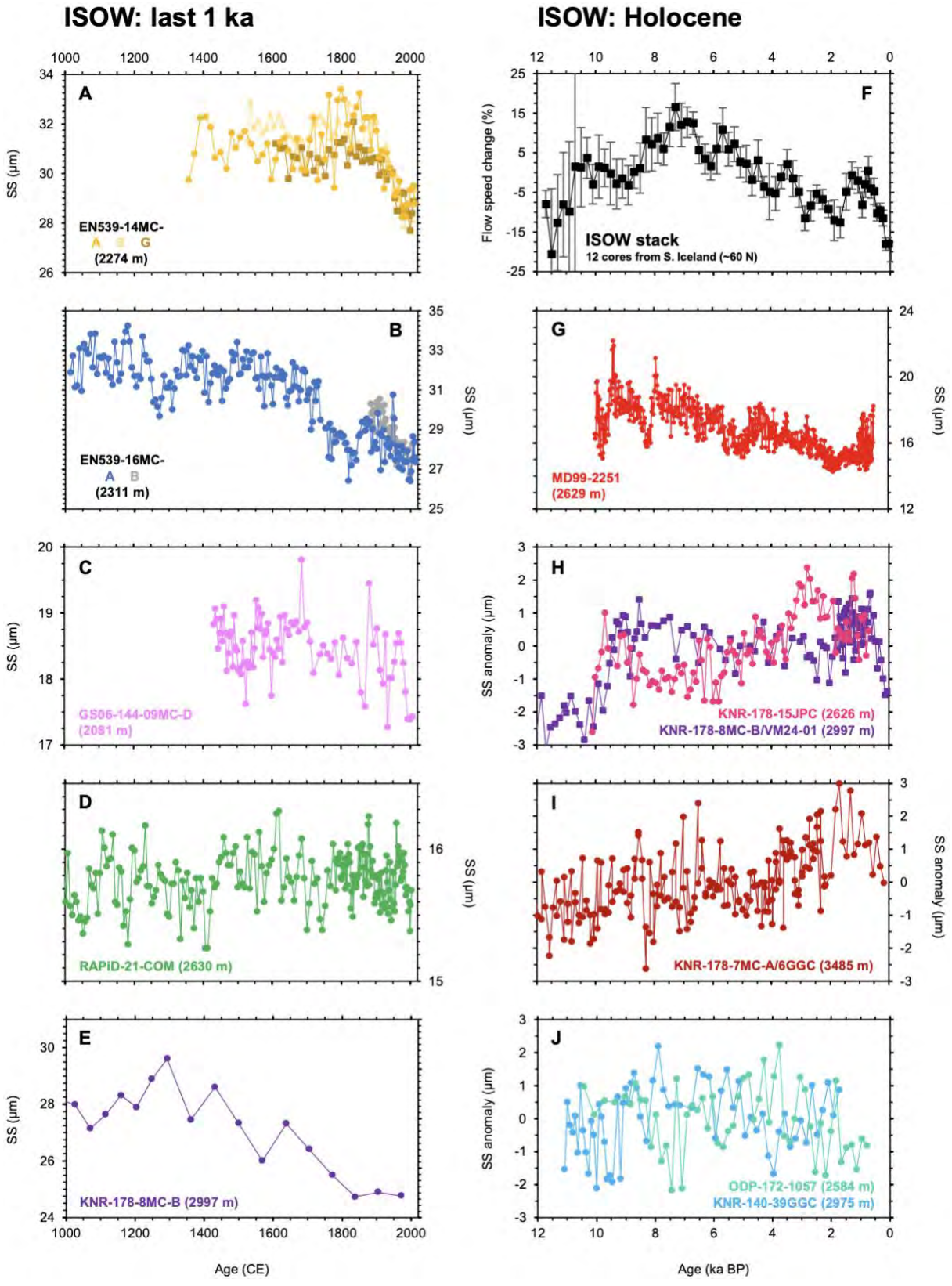

Figure 5. Compilation of grain size records from cores predominantly influenced by ISOW in the subpolar Northwest Atlantic and NEADW in the Northwest Atlantic for the last ~1 ka (left panels) and Holocene (right panels). (a) EN359-14MC-A (yellow circles), -B (gold triangles), and -G (brown squares); (b) EN359-16MC-A (blue) & -B (grey); (c) GS06-144-09MC-D (Mjell et al., 2016; pink); (d) RAPiD-21-COM (Moffa-Sanchez et al., 2017; green); (e) KNR-178-8MC-B (purple); (f) ISOW flow speed change stack (black)

with standard error bars (±2SE); (f) MD99-2251 (Hoogakker et al., 2010; red); (h) SS anomalies for KNR-178-15JPC (pink) & KNR-178-8MC-B/VM24-01 (purple); (i) SS anomalies for KNR-178-7MC-A/6GGC (dark red); (j) SS anomalies for BOR cores ODP-172-1057 (turquoise) and KNR-140-39GGC (light blue).

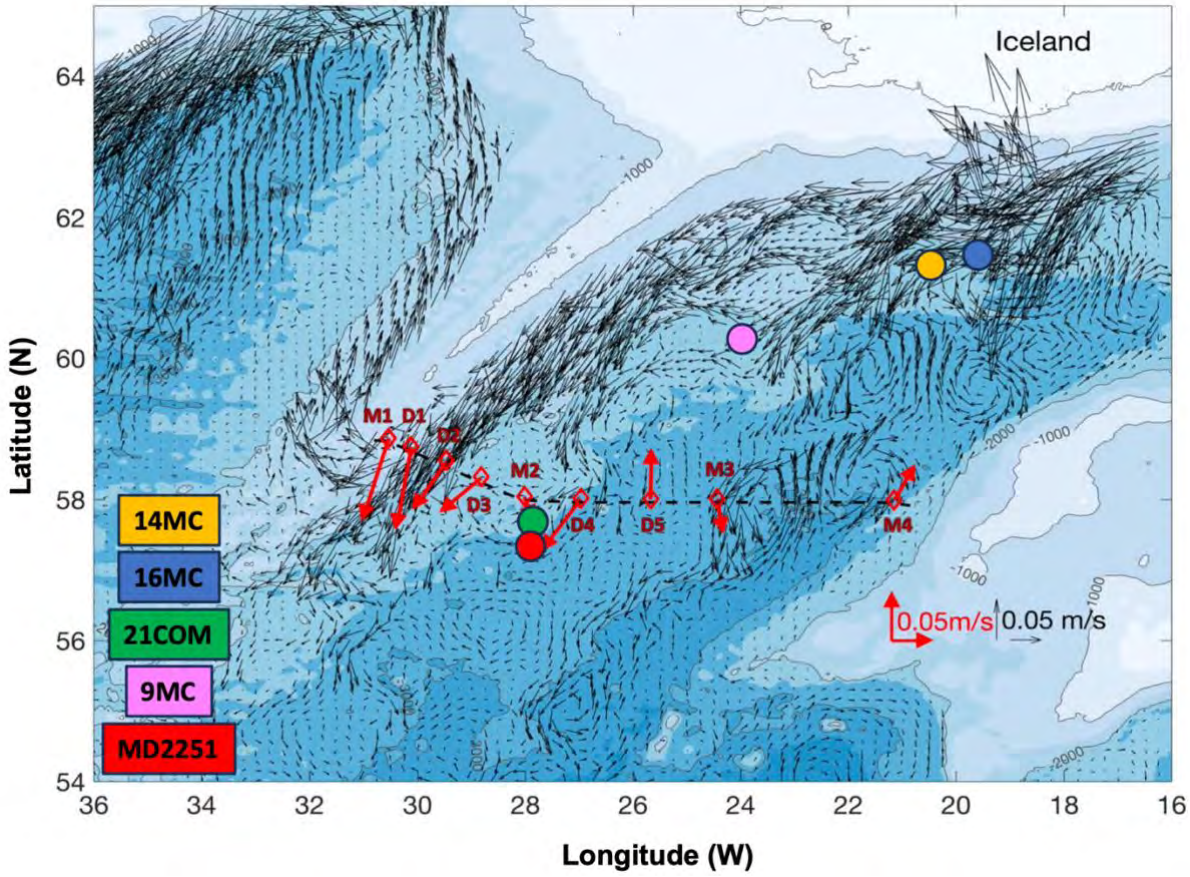

Figure 6. Modelled fifteen-year mean currents (black arrows), with OSNAP 4-year mean currents overlaid (in red), averaged over the density layer σ_θ > 27.8. Coloured circles denote the position of cores featured in our ISOW grain size compilations. Adapted from Johns et al., (2021).

2.2.2 Holocene (11.7-0 ka BP)

We have updated the Holocene ISOW stack from Thornalley *et al.*, (2013) by adding new records and improving the resolution of existing cores, e.g., EW9302-25GGC, EW9302-26GGC, and EW9302-29GGC. Overall, the Holocene trend remains unchanged, i.e., a long-term decrease over the last ~7 ka. However, the addition of new data helps to resolve millennial-scale variability throughout the Holocene. Further downstream, grain size records spanning between ~2.5 and ~3.5 km at Cape Hatteras and Blake Outer Ridge show limited downcore coherence and do not resolve the long-trend decrease evident in the Iceland Basin ISOW stack suggesting that ISOW does not maintain the same depth in the Northwest Atlantic throughout the Holocene. All Holocene data corresponding ISOW depths is presented in Figure 5 and the main results are as follows:

- Updated ISOW stack derived from a suite of cores spanning between 1.2 and 2.4 km water depth reveal a long-term reduction in inferred flow speeds over the last ~7 ka, with persistent millennial-scale variability throughout (Figure 5f).
- Gardar Drift core MD2251 shows little similarity to the update ISOW stack (Figure 5g), most likely due to systematic methodological error (ongoing work has highlighted how the data

corresponding to between 7.5 and 9 ka BP is not reproducible [Hewitt *et al.,* 2022; International Conference on Paleoceanography poster).

- Cape Hatteras cores spanning between 2.5 and 3.5 km water also show little long-term similarity with the updated ISOW stack (Figure 5h and 5i).
- In particular, the shallowest site, 15JPC, shows a gradual increase between ~8 and ~2 ka BP, more reminiscent of Holocene LSW variability, which could be driving the record instead. For example, Cape Hatteras is a crossover region, where LSW is subducted beneath the Gulf Stream resulting in LSW occupying greater depths at these latitudes.
- In comparison, deeper core, 6GGC shows an uptick over the last ~2 ka, which could be related to a shoaling of the underlying DSOW.
- Blake Outer Ridge cores from ~2.5-3 km water also bear little resemblance to the updated ISOW stack (Figure 5j); however, it should be noted that cores from similar depths at Cape Hatteras and Blake Outer Ridge show very good downcore agreement prior to ~4 ka BP, e.g., 8MC and 39GGC (Figure 7).

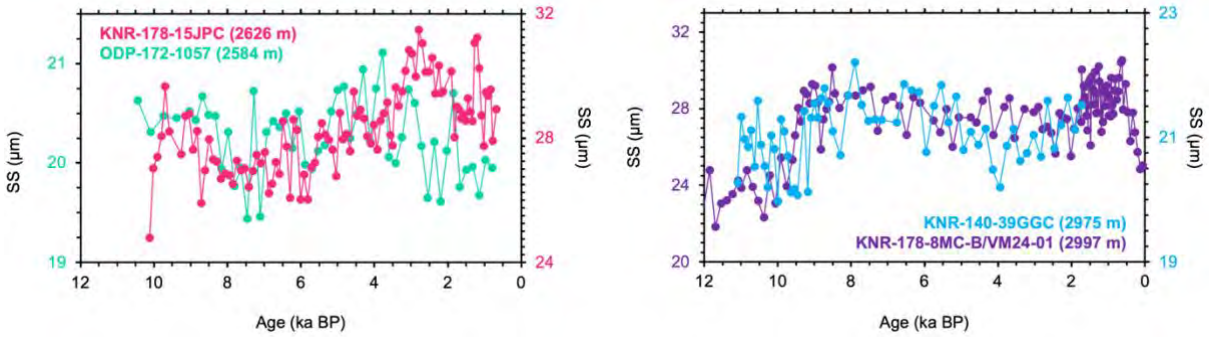

Figure 7. Comparison of grain size records from cores at similar water depths at Cape Hatteras and Blake Outer Ridge (a) KNR-178-15JPC vs ODP-172-1055, and (b) KNR-178-8MC-B/VM24-01 vs KNR-140-39GGC (Evans & Hall, 2008).

2.3 Denmark Strait Overflow Water (DSOW)

DSOW is sourced primarily from a combination of (1) waters formed via deep ocean convection in the Nordic Seas and (2) Atlantic inflow water that cools and sinks as it circulates cyclonically around the boundary of the Nordic Seas basin (Isachsen et al., 2007; Hansen & Østerhus, 2007). Like ISOW, DSOW enters the North Atlantic by overflowing the GSR, but further northwest via the Denmark Strait. After descending into the Atlantic Basin, DSOW joins up with ISOW in the southern Irminger Sea, before flowing cyclonically around the Labrador Sea, eventually joining up with LSW to form the DWBC. Despite its relative freshness compared to ISOW, DSOW's associated colder temperatures result in it being denser, and thus it underlies ISOW, typically occupying water depths between ~3.5 and ~4.5 km throughout the Northwest Atlantic.

Compared to LSW and ISOW, DSOW reconstructions are more limited. However, previous work suggests there has been a gradual increase in DSOW strength during the Mid to Late-Holocene (Kleiven *et al.,* 2008; Moffa-Sanchez *et al.,* 2015). In this section, we present and examine new DSOW grain size records, as well as building directly on previously published records (Moffa-Sanchez *et al.,* 2015; Table 3; Figure 8). Since high resolution records of DSOW spanning the last ~1 ka are rare, we divide our analyses between records covering the Holocene and last ~2 ka, so as to enable better spatial coverage of past DSOW variability. Furthermore, despite including core 6GGC in our ISOW-Holocene analyses, on more recent timescales this site seems likely to have been more influenced by DSOW. Thus, we also include 6GGC in the following DSOW-last 2 ka compilation.

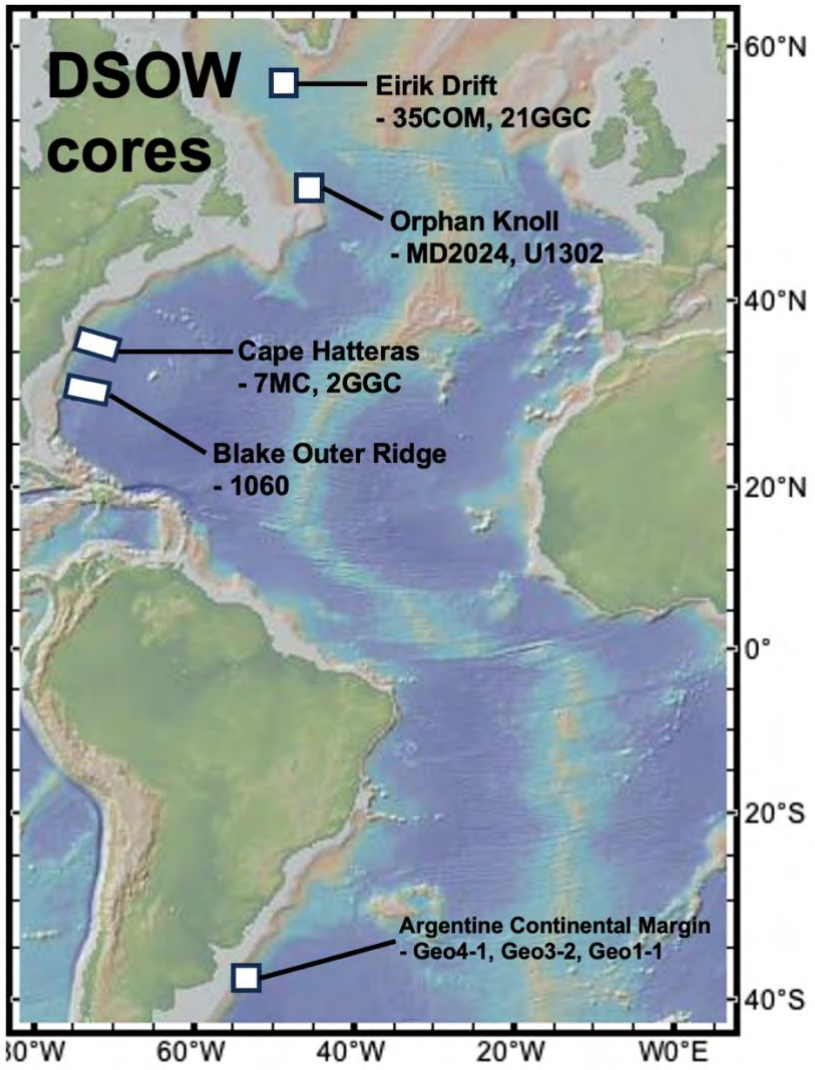

Figure 8. Site map showing location of cores detailed in Table 3. Squares denote sites with multiple cores and rectangles denote paleoenvironmental depth transects.

Table 3. Details of cores corresponding to typical DSOW depths.

Core and (abbreviation)	Region	Lat. (N)	Long. (W)	Depth (m)	Duration	Reference
RAPiD-35-COM (35COM)	Eirik Drift	57.50	48.72	3484	2 ka/Hol.	Moffa-Sanchez *et al.*, 2015; this report
KNR-166-21GGC (21GGC)	Eirik Drift	57.44	48.61	3471	2ka/Hol.	Henderson, 2009
HU91-045-093/MD95-2024 (MD2024)	Orphan Knoll	50.19	45.66	3448	2 ka/Hol.	This report
KNR-178-2GGC (2GGC)	Cape Hatteras	36.12	72.29	3927	2 ka/Hol.	This report

IODP-U1302	Orphan Knoll	50.19	45.66	3559	Holocene	This report
ODP-172-1060	BOR	30.77	74.47	3481	Holocene	This report
GeoB13824-1 (Geo4-1)	Necochea Terrace	-38.22	53.35	3821	Holocene	Warratz *et al.*, 2017
GeoB13823-2 (Geo3-2)	Necochea Terrace	-38.14	53.34	3780	Holocene	Warratz *et al.*, 2017
GeoB13861-1 (Geo1-1)	Mar de Plata Canyon	-38.09	53.61	3715	Holocene	Warratz *et al.*, 2017

2.3.1 Last 2 ka

Grain size records corresponding to DSOW variability over the last ~2 ka show little long-term change, although low resolution records from Cape Hatteras suggest a slight decline. These data are presented in Figure 9 and the main findings are summarised below:

- Updated grain size record 35COM and 21GGC from Eirik Drift in the Labrador Sea shows little long-term change in grain size over the last ~1 ka (Figure 9a).
- Similarly, MD2024, from further downstream at Orphan Knoll, exhibits long-term change in grain size over the last ~1 ka (Figure 9b).
- Since we see some coherence at ISOW depths between Cape Hatteras and sites in the Iceland Basin, we also might expect to see similar coherence between Cape Hatteras and sites from further upstream at DSOW depths. Low resolution records from Cape exhibits long-term change in grain size over the last ~1 ka (Figure 9c), although a slight decrease is recorded in the shallower core 6GGC/7MC (3485m), which could be related to the weakening of ISOW seen at Cape Hatteras core 8MC (2997m). Testing whether these minor shifts at depth could be caused by DSOW and ISOW variability, and/or vertical shifts in DSOW/ISOW presents another target for future modelling work as part of EPOC.

2.3.2 Holocene

Overall, grain size records corresponding to DSOW variability during the Holocene all show fastest inferred flow speeds during an Early-Holocene peak. However, records from the Labrador Sea, have a pronounced early Early-Holocene peak, followed by a long-term increase after ~8 ka BP, whereas other regions show a long-term decline throughout the mid-late Holocene. These differences could be due to:

1. **The influence of the subpolar gyre on the Labrador Sea records**
2. **Shoaling of DSOW during the Late Holocene**
3. **Mixing of ISOW and DSOW at subtropical latitudes**

We present Holocene data corresponding to depths likely influenced by DSOW in Figure 9 and summarise the key findings below:

- Grain size records from Eirik Drift and Orphan Knoll are all characterized by a very strong Early-Holocene and gradual Mid to Late-Holocene increase (Figure 9d and 9e).
- Further downstream at Cape Hatteras and Blake Outer Ridge, grain size records exhibit a long-term decline after the period of Early-Holocene strength (Figure 9f).

- Much further south, at the Argentine Continental Margin, three grain size records from between ~3 and 4 km water depth also all exhibit very high values during the Early-Holocene (Warratz *et al.,* 2017; Figure 9g). Although currently bathed by AABW, it is possible that the strong early Holocene flow speeds relate to a period of stronger DSOW flow reaching this site via the DWBC.

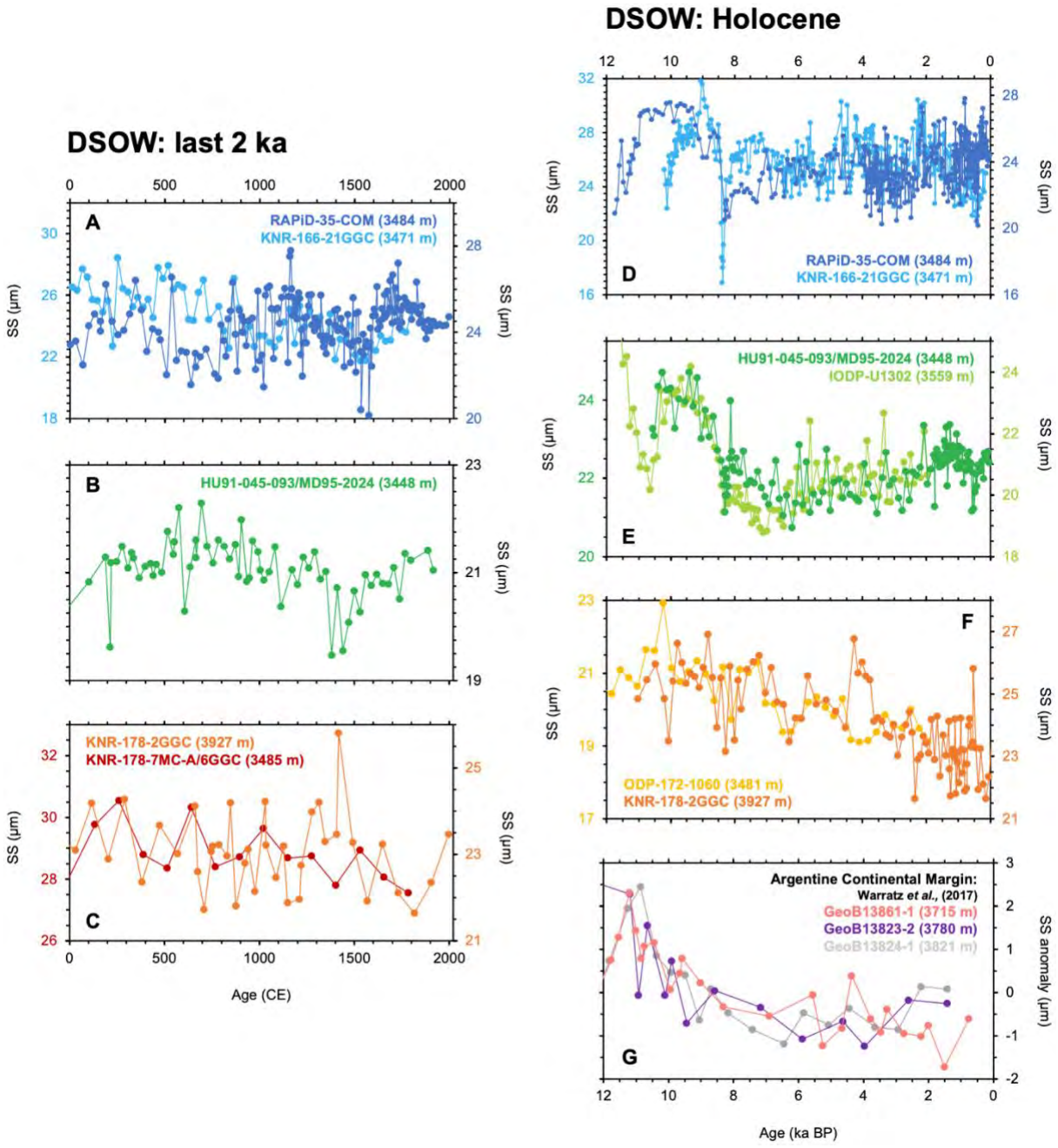

Figure 9. Compilation of grain size records from cores predominantly influenced by DSOW for the last ~2 ka (left panels) and Holocene (right panels). (a) & (d) Eirik Drift cores - RAPiD-35-COM (blue) & KNR-166-21GGC (light blue); (b) HU91-045-09/MD95-2024 (green); (c) KNR-178-7MC/6GGC (dark red) & KNR-178-2GGC (orange); (e) Orphan Knoll cores - HU91-045-09/MD95-2024 (green) & IODP-1302 (lime); (f) ODP-172-1060 (yellow) & KNR-178-2GGC (orange); (g) Argentine Continental Margin cores (Warratz et al., 2017) – GeoB13861-1 (light red), GeoB13823-2 (purple), & GeoB13824-1 (grey).

3 North Atlantic benthic foraminiferal $\delta^{18}O_c$ records

The ratio of oxygen-16 to oxygen-18 preserved in the calcitic tests of benthic foraminifera, i.e., $\delta^{18}O_c$, is a conservative water mass tracer that can be used to trace the source and mixing of deep water masses. In this section, we present a selection of new and ~1 ka long $\delta^{18}O_c$ records from sediments cores in the Northwest Atlantic, most of which were already featured in Section 2. Although $\delta^{18}O_c$ reflects both the temperature and $\delta^{18}O$ of seawater, the latter of which is highly correlated with salinity, here we leverage the conservative nature of $\delta^{18}O_c$, i.e., that it is only influenced by mixing between water masses (assuming negligible temperature effects due to geothermal and pressure heating), to provide insight into the vertical and latitudinal coherence of the AMOC's constituent water masses. In keeping with Section 2, we divide these records between those bathed by LSW or ISOW/NEADW, using both absolute $\delta^{18}O_c$ values and water depth to make this distinction.

3.1 LSW

Benthic $\delta^{18}O_c$ records from <2 km water depth are typically centred at ~2.65 ‰ and characterized by a long-term increase from ~1000 CE followed by a more abrupt increase starting at some point after ~1650 CE, both of which suggest that the same water mass, i.e., LSW, is bathing these sites from Newfoundland to Cape Hatteras. These latter changes are broadly consistent with published records from the North Atlantic that suggest major changes in surface and deep ocean circulatory regimes starting at ~1850 CE (Keigwin *et al.,* 2003; Moore *et al.,* 2017; Lower-Spies *et al.,* 2020; Spooner *et al.,* 2020). We present these new data in full in Figure 10 and summarise the main results below:

- 10MC is characterized by a long-term increase in $\delta^{18}O_c$ between ~1000 CE and ~1750 CE, followed by reversal to lower values (Figure 10a). While this is broadly consistent with evidence from a model inversion (Gebbie, 2019), our records show a reversal to lower values much earlier. We suggest that this may be caused by increased freshwater input in the Labrador Sea at the end of the Little Ice Age, as well as warmer temperatures associated with the Industrial Era post ~1900 CE (Thornalley *et al.,* 2018; Gebbie, 2019).
- 56JPC also shows a relatively abrupt decrease in $\delta^{18}O_c$ post ~1750 CE (Figure 10b). Given the likely influence of LSW at both 10MC and 56JPC, we suggest this variability is also driven by a combination of freshwater and/or Industrial Era warmth.
- Although relatively low-resolution (note that we have resampled this core and will be increasing the data resolution by fivefold), core 82A generally exhibits similar behaviour to 10MC and 56JPC (Figure 11), however, we note that the absolute values are much higher (0.1-0.2 ‰). Additional work, both modelling and proxy investigation, is required in order to reconcile this difference. In particular, additional analyses are required in order to rule out potential secondary controls, e.g., the carbonate ion effect, on benthic foraminiferal test chemistry at this site.

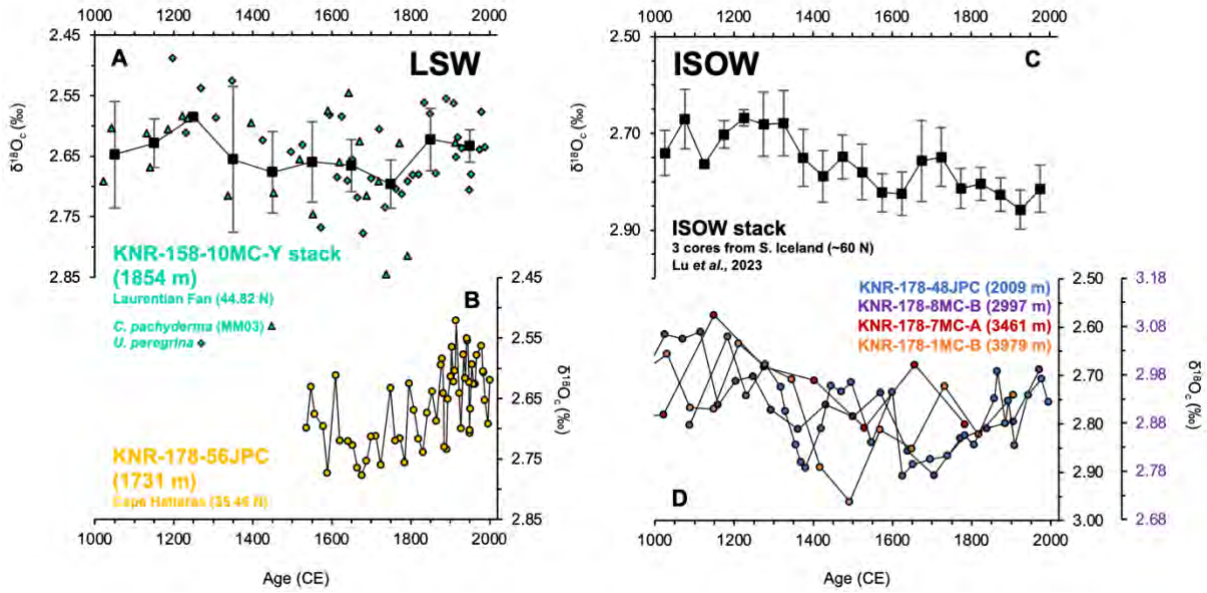

Figure 10. Compilation of benthic foraminiferal $\delta^{18}O$ from cores predominantly influenced by LSW (left panels) and ISOW/NEADW (right panels) for the last 1 ka. (a) Multi-species KNR-158-10MC-Y stack (black squares) with standard error (±2SE); (b) KNR-178-456JPC – benthic $\delta^{18}O_c$ values are from U. peregrina (and offset of -0.7 ‰ has been applied to correct for species-specific vital effects); (c) ISOW stack based on three cores from South of Iceland (Lu et al., 2023; EN539-9MC-A, EN539-13MC-A; EN539-14MC-A); (d) Cape Hatteras cores – KNR-178-48JPC (blue), KNR-178-8MC-B (purple), KNR-178-7MC-A (dark red), & KNR-178-1MC-B (orange). Note the different y-axis for KNR-178-8MC-B. All benthic $\delta^{18}O_c$ are from Cibicidoides spp. unless otherwise stated.

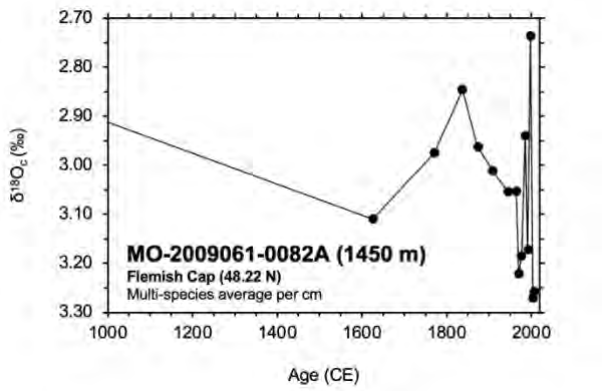

Figure 11. Benthic foraminiferal $\delta^{18}O$ for Flemish Pass core MO-2009061-0082A. Note that these data are based on the multi-species average $\delta^{18}O_c$ for each cm (benthic foraminiferal $\delta^{18}O$ is from Noniella labradorica, Melonis affinis, Elphidium excavatum, and Cibicidoides spp.).

3.2 ISOW/NEADW

Benthic $\delta^{18}O_c$ records from between ~2 and 4 km along the North American continental margin generally show good inter-site agreement over the last ~1 ka, both in terms of absolute values (centred at ~2.8 ‰) and long-term trends. Collectively, this suggests that each of these sites is being influenced by the same deep ocean water mass, but one that is geochemically distinct from LSW above. These Northwest Atlantic records also show similar long-term behaviour to a suite of records from South of Iceland that are recording ISOW variability. This is in terms of both absolute values, and long-term trends, although the former is of a lesser magnitude and

the exact timing of change to lower values happens earlier at Cape Hatteras than further upstream in the Iceland Basin. We present these novel $\delta^{18}O_c$ in Figure 10 and summarise the key findings below:

- Benthic $\delta^{18}O_c$ records from Cape Hatteras spanning between ~2 and 4 km all exhibit the same broad trend over the last ~1 ka (Figures 10d), i.e., a long-term increase (note the reversed axes for $\delta^{18}O_c$) followed by a decrease over the last ~200 years.
- However, it should be noted that the exact timing of these changes varies slightly between cores, likely due to limited resolution and dating.
- Apart from 8MC, absolute benthic $\delta^{18}O_c$ values show good agreement, which suggests they are being bathed by the same water mass.
- In terms of absolute values, benthic $\delta^{18}O_c$ records from Cape Hatteras also show good agreement with a suite of benthic $\delta^{18}O_c$ records from South of Iceland that are predominantly influenced by ISOW (Figure 10c), however, we note the exact timing of changes in the cores from the two regions differ slightly. We hypothesize that these broad similarities over the last ~1 ka are due to common basin-wide surface ocean changes being transmitted into the deep ocean via both overflows, as well as LSW.
- Compared to 56JPC at 1731m water depth, 48JPC at 2009m is ~0.15-0.2 ‰ heavier, which suggests that the water mass boundary between LSW and ISOW is situated between these two depths at Cape Hatteras.

4 Summary

In this section we summarise the main findings of both previous paleo proxy compilations, as well as the main points related to our new deep ocean records.

4.1 Caesar *et al.,* (2021) – Current AMOC weakest in last millennium

This compilation presents a series of proxy records that reconstruct the evolution of AMOC since 400 CE, including:

- SST-based proxies, which are inferred as the North Atlantic temperaure response to AMOC change (Caesar *et al.,* 2018; Rahmstorf *et al.,* 2015; Thornalley *et al.,* 2018).
- Indicators of local marine productivity, e.g., $\delta^{15}N$ (Sherwood *et al.,* 2011) and methanesulfonic acid concentration in Greenland ice cores (Osman *et al.,* 2019)
- Sortable silt mean grain size data (Thornalley *et al.,* 2018).
- Benthic foraminiferal $\delta^{18}O$ (Thibodeau *et al.,* 2018) and the relative abundance of the planktic foraminifera, *T. quinqueloba* (Spooner *et al.,* 2020), both of which are proxies for the relative regional changes in Atlantic heat content.

The main findings are detailed below:

- Prior to ~1800 CE, all proxy records examined in this study are relatively invariable, which suggests that the AMOC was also relatively stable over this time period.
- In comparison, post ~1800 CE, all proxy records show a decline. In particular, around 1960 CE, several proxies indicate a period of rapid decline, followed by a period of recovery in the 1990s, and additional decline during the 2000s.

- All proxies resolve multi-decadal scale variability, although this is often incoherent in terms of magnitude and timing, which may be due non-AMOC related influences.

4.2 Moffa-Sanchez *et al.,* (2019) – Variability in the Northern North Atlantic and Arctic Oceans across the last two millennia: a review

This work presents a relatively exhaustive compilation of high-resolution paleoceanographic datasets available in 2019 and discusses them by region at great length (see their Section 7 for a summary). However, this work did not individually assess the validity of each of these records as a potential AMOC proxy. Therefore, to enable this analysis, which deals specifically with this task as part of WP3, we have collated these records (alongside other complementary ones published since 2019) and pass them forward in the accompanying Excel file.

4.3 Summary of this report's main findings

Results in this report supplement these previous studies and are summarised below. Furthermore, we combine these published data with our new sortable silt and benthic δ^{18}Oc data, as well as newly published records in the attached excel file, which forms part of the focus of WP3.

4.3.1 Last 1 ka

- Grain size records of LSW variability show a range of different behaviour over the last 1 ka. However many records show notable changes post ~1800 CE.
- Grain size records of ISOW variability from South of Iceland to Cape Hatteras also exhibit major changes post ~1800 CE, in particular, a decline in inferred flow speeds, which suggests ISOW flow may be somewhat latitudinally coherent on multi-decadal timescales.
- Benthic foraminiferal δ^{18}Oc records from the North Atlantic all generally exhibit similar behaviour over the last 1 ka, namely a long-term decrease prior to ~1700 CE, followed by a more abrupt increase. However, the exact timing of this change varies between cores from the Iceland Basin and the Northwest Atlantic, e.g., Cape Hatteras.
- Benthic δ^{18}Oc records from Northwest Atlantic cores also reveal a clear water mass boundary between LSW and ISOW/NEADW between ~1.7 and 2 km water depth.
- In comparison, grain size records from >3.5 km water depth are less coherent over the last 1 ka.

4.3.2 Holocene

- On millennial timescales, grain size records corresponding to LSW flow speed variability generally show a long-term increase over the last ~8 ka.
- Building on previous work (Thornalley *et al.,* 2013), we infer that ISOW strength has decreased over the last ~8 ka, whilst also experiencing persistent shorter-term variability. However, unlike LSW, grain size records from the Northwest Atlantic at depths currently bathed by ISOW generally show differing behaviour.
- Similarly, grain size records from >3.5 km depth, which is strongly influenced by DSOW in the Northwest Atlantic, show differences between the Labrador Sea and Cape Hatteras.

- Both these latter points highlight that on long timescales it seems likely that there have been vertical shifts in the positions of all three major water masses. This is something that is important to constrain when looking at models and proxy data on millennial timescales.

4.4 Recommendations for proxy-model comparisons as part of EPOC WP3

- Examination of LSW's vertical and latitudinal coherence on decadal-to-centennial timescales.
- Where we see differences in flow speeds from cores retrieved from similar depths, is it possible to determine whether these changes are likely related to vertical shifts in components of the DWBC and/or latitudinal differences?
- Are ISOW and DSOW latitudinally coherent on decadal-to-centennial timescales, especially when relating to externally forced responses?

5 References

Bianchi, G. G., & McCave, I. N. (1999) 'Holocene periodicity in North Atlantic climate and deep-ocean flow south of Iceland', *Nature*, 397, 6719, 515-517.

Buckley M.W. & J. Marshall (2016) 'Observations, inferences and mechanisms of the Atlantic meridional overturning circulation: a review', *Reviews of geophysics*, 54, 5-63.

Caesar, L., Rahmstorf, S., Robinson, A., Feulner, G. & V. Saba (2018) 'Observed fingerprint of a weakening Atlantic Ocean overturning circulation', *Nature*, 566, 191-196.

Caesar, L., McCarthy, G.D., Thornalley, D.J.R, Cahill, N. & S. Rahmstorf (2021) 'Current Atlantic Meridional Overturning Circulation weakest in last millennium', *Nature Geoscience,* 14, 118-120.

Evans, H. K., & Hall, I. R. (2008) 'Deepwater circulation on Blake Outer Ridge (western North Atlantic) during the holocene, younger dryas, and last glacial maximum', *Geochemistry, Geophysics, Geosystems*, 9, 3.

Gebbie, G. (2019) 'Atlantic warming since the Little Ice Age', *Oceanography*, 32, 1, 220-230.

Girard-Sequeira, A (2023) 'Deconvoluting the effects of marine bioturbation in the last 150 years; a new insight into Anthropogenic impact on the Labrador Current', *MSc thesis*, 1-73.

Hansen, B., & Østerhus, S. (2007) 'Faroe bank channel overflow 1995–2005', *Progress in Oceanography*, 75, 4, 817-856.

Henderson, S.S (2009) 'Tracking deep-water flow on Eirik Drift over the past 160 kyr: linking deep-water changes to freshwater fluxes, *PhD Thesis*, 1-160.

Hewett, Z, Thornalley, D.J.R, Oppo, D., Hall, I., & D. Wilson (2023) 'A reassessment of the palaeoceanographic evidence for changes in the deep branches of North Atlantic circulation during the 8.2 kyr event', Conference Poster: PAC2023

Hoffmann, S. S., Dalsing, R. E., & Murphy, S. C. (2019) 'Sortable silt records of intermediate-depth circulation and sedimentation in the Southwest Labrador Sea since the Last Glacial Maximum', *Quaternary Science Reviews*, 206, 99-110.

Hoogakker, B., Elderfield, H., Oliver, K., & Crowhurst, S. (2010) 'Benthic foraminiferal oxygen isotope offsets over the last glacial-interglacial cycle', *Paleoceanography*, 25, 4.

Hoogakker, B. A., Chapman, M. R., McCave, I. N., Hillaire-Marcel, C., Ellison, C. R., Hall, I. R., & Telford, R. J. (2011) 'Dynamics of North Atlantic deep water masses during the Holocene', *Paleoceanography*, 26, 4.

Isachsen, P. E., Mauritzen, C., & Svendsen, H. (2007) 'Dense water formation in the Nordic Seas diagnosed from sea surface buoyancy fluxes', *Deep Sea Research Part I: Oceanographic Research Papers*, *54*(1), 22-41.

Johns, W. E., Devana, M., Houk, A., & Zou, S. (2021) 'Moored Observations of the Iceland-Scotland Overflow Plume Along the Eastern Flank of the Reykjanes Ridge', *Journal of Geophysical Research: Oceans*, 126, 8, e2021JC017524.

Keigwin, L.D., Sachs, J.P. & Y. Rosenthal (2003) 'A 1600-year history of the Labrador Current off Nova Scotia', *Climate Dynamics,* 21, 53-62.

Kissel, C., Van Toer, A., Laj, C., Cortijo, E., & Michel, E. (2013) 'Variations in the strength of the North Atlantic bottom water during Holocene', *Earth and Planetary Science Letters*, 369, 248-259.

Lazier, J., Hendry, R., Clarke, A., Yashayaev, I., & Rhines, P. (2002) 'Convection and restratification in the Labrador Sea, 1990–2000', *Deep Sea Research Part I: Oceanographic Research Papers*, 49, 10, 1819-1835.

Lower-Spies, E. E., Whitney, N. M., Wanamaker, A. D., Griffin, S. M., Introne, D. S., & Kreutz, K. J. (2020) 'A 250-year, decadally resolved, radiocarbon time history in the Gulf of Maine reveals a hydrographic regime shift at the end of the Little Ice Age', *Journal of Geophysical Research: Oceans*, *125*(9), e2020JC016579.

Lozier, M. S., Bower, A. S., Furey, H. H., Drouin, K. L., Xu, X., & Zou, S. (2022) 'Overflow Water Pathways in the North Atlantic', *Progress in Oceanography*, 102874.

Marchitto, T.M. & P.B. deMenocal (2003) 'Late Holocene variability of upper North Atlantic Deep-Water temperature and salinity', *Geochemistry, geophysics, geosystems,* 4, 12, 1100, doi:10.1029/2003GC000598.

Menary *et al.*, (2020) 'Aerosol-Forced AMOC Changes in CMIP6 Historical Simulations', *Geophysical Research Letters*, 47, e2020GL088166. https://doi. org/10.1029/2020GL088166

Mjell, T. L., Ninnemann, U. S., Eldevik, T., & Kleiven, H. K. F. (2015) 'Holocene multidecadal-to millennial-scale variations in Iceland-Scotland overflow and their relationship to climate', *Paleoceanography*, 30, 5, 558-569.

Mjell, T. L., Ninnemann, U.S., Kleiven, H.F., & I. R. Hall (2016) 'Multidecadal changes in Iceland Scotland Overflow Water vigor over the last 600 years and its relationship to climate', *Geophysical Research Letters*, 43, 2111–2117, doi:10.1002/ 2016GL068227.

Moat B.I. Smeed D.A.; Rayner D.; Johns W.E.; Smith, R.; Volkov, D.; Baringer M. O.; and Collins, J. (2023). Atlantic meridional overturning circulation observed by the RAPID-MOCHA-WBTS (RAPID-Meridional Overturning Circulation and Heatflux Array-Western Boundary Time Series) array at 26N from 2004 to 2022 (v2022.1), British Oceanographic Data Centre - Natural Environment Research Council, UK. doi: 10.5285/04c79ece-3186-349a-e063-6c86abc0158c.

Moffa-Sánchez, P., Hall, I. R., Barker, S., Thornalley, D. J., & Yashayaev, I. (2014) 'Surface changes in the eastern Labrador Sea around the onset of the Little Ice Age', *Paleoceanography*, 29, 3, 160-175.

Moffa-Sanchez, P., Hall, I. R., Thornalley, D. J., Barker, S., & Stewart, C. (2015) 'Changes in the strength of the Nordic Seas Overflows over the past 3000 years', *Quaternary Science Reviews*, 123, 134-143.

Moffa-Sánchez, P., & Hall, I. R. (2017) 'North Atlantic variability and its links to European climate over the last 3000 years', *Nature Communications*, 8, 1, 1-9.

Moffa-Sánchez, P., Moreno-Chamarro, E., Reynolds, D. J., Ortega, P., Cunningham, L., Swingedouw, D., ... & Yeager, S. (2019) 'Variability in the northern North Atlantic and Arctic oceans across the last two millennia: A review', *Paleoceanography and Paleoclimatology*, 34, 8, 1399-1436.

Moore, G. W. K., Halfar, J., Majeed, H., Adey, W., & Kronz, A. (2017) 'Amplification of the Atlantic Multidecadal Oscillation associated with the onset of the industrial-era warming', *Scientific Reports*, 7, 1, 1-10.

O'Brien, C. L., Spooner, P. T., Wharton, J. H., Papachristopoulou, E., Dutton, N., Fairman, D., ... & Thornalley, D. J. (2021) 'Exceptional 20th century shifts in deep-sea ecosystems are spatially heterogeneous and associated with local surface ocean variability', *Frontiers in Marine Science*, 1376.

Osman, M. B., Das, S. B., Trusel, L. D., Evans, M. J., Fischer, H., Grieman, M. M., ... & Saltzman, E. S. (2019) 'Industrial-era decline in subarctic Atlantic productivity', *Nature*, 569, 7757, 551-555.

Petit, T., Lozier, M. S., Josey, S. A., & Cunningham, S. A. (2020) 'Atlantic deep water formation occurs primarily in the Iceland Basin and Irminger Sea by local buoyancy forcing', *Geophysical Research Letters*, 47, 22, e2020GL091028.

Piper, D. J., Li, G., Andrews, J. T., Jennings, A. E., & Robertson, L. (2021) 'Transport of fine-grained sediment in oceanic currents: Holocene supply to sediment drifts around Flemish Cap by the Labrador Current', *Marine Geology*, 436, 106494.

Rahmstorf, S., Box, J.E., Feulner, G., Mann, M.E., Robinson, A., Rutherford, S. & E.J. Schaffernicht (2015) 'Exceptional twentieth-century slowdown in Atlantic Ocean overturning circulation', *Nature Climate Change*, 5, 475-480.

Rashid, H., Zhang, Z., Piper, D. J., Patro, R., & Xu, Y. (2023) 'Impact of Medieval Climate Anomaly and Little Ice Age on the Labrador Current flow speed and the AMOC reconstructed by the sediment dynamics and biomarker proxies', *Palaeogeography, Palaeoclimatology, Palaeoecology*, *620*, 111558.

Renssen, H., Goosse, H., & T. Fierefet (2005) 'Contrasting trends in North Atlantic deep-water formation in the Labrador Sea and Nordic Seas during the Holocene', *Geophysical Research Letters*, 32, L08711, doi:10.1029/2005GL022462.

Sherwood *et al.,* (2011) 'Nutrient regime shift in the western North Atlantic indicated by compound-specific $\delta^{15}N$ of deep-sea gorgonian corals', *PNAS*, 108, 3, 1011-1015.

Spooner, P. T., Thornalley, D. J., Oppo, D. W., Fox, A. D., Radionovskaya, S., Rose, N. L., ... & Roberts, J. M. (2020) 'Exceptional 20th century ocean circulation in the northeast Atlantic', *Geophysical Research Letters*, 47, 10, e2020GL087577.

Srokosz, M.A. & H. L. Bryden (2015) 'Observing the Atlantic Meridional Overturning Circulation yields a decade of inevitable surprises', *Science*, 348, 6241, 1330-1335.

Thibodeau, B., Not, C., Zhu, J., Schmittner, A., Noone, D., Tabor, C., ... & Liu, Z. (2018) 'Last century warming over the Canadian Atlantic shelves linked to weak Atlantic meridional overturning circulation', *Geophysical Research Letters*, 45, 22, 12-376.

Thornalley, D. J., Blaschek, M., Davies, F. J., Praetorius, S., Oppo, D. W., McManus, J. F., ... & McCave, I. N. (2013) 'Long-term variations in Iceland–Scotland overflow strength during the Holocene', *Climate of the Past*, 9, 5, 2073-2084.

Thornalley, D.J.R., Oppo, D.W., Ortega, P., Robson, J.I., Brierley, C.M., Davis, R., Hall, I.R., Keigwin, L.D., Moffa-Sanchez, P., Rose, N.L., Spooner, P.T. & I. Yashayaev (2018) 'Anomalously weak Labrador Sea convection and Atlantic overturning during the last 150 years', Nature, 566, 227-230.

Warratz, G *et al.,* (2017) 'Deglacial changes in the strength of deep southern component water and sediment supply at the Argentine continental margin', *Paleoceanography*, 32, 8, 796-812, https://doi.org/10.1002/2016PA003079

Weitzman, J., Ledger, S., Stacey, C.D., Strathdee, G., Piper, D.J.W., Jarrett, K.A., Higgins, J., (2014) '*Logs of short push cores, deep-water margin of Flemish Cap and the eastern Grand Banks of Newfoundland'*, Geol. Surv, Canada Open File 7148.